Bulgarian Chemical Communications, Volume 55, Issue 2 (pp. 133-138) 2023 DOI: 10.34049/bcc.55.2.NC05

Dielectric characterization (complex electric modulus) of Na^+-ion conducting PEO/E8/$NaIO_4$ salt-complexed polymer/liquid crystals composite

T. E. Vlakhov, Y. G. Marinov, G. B. Hadjichristov*

Georgi Nadjakov Institute of Solid State Physics, Bulgarian Academy of Sciences, 72 Tzarigradsko Chaussee Blvd., BG-1784 Sofia, Bulgaria

Received: July 26, 2022; Revised: March 21, 2023

The frequency behavior (in the range 1 Hz – 1 MHz) of the complex electric modulus of flexible films (150 μm-thick) of Na^+-ion conducting composite electrolyte produced from polymer poly(ethylene oxide) (PEO), nematic liquid crystals E8 and the salt $NaIO_4$ (in compositional ratio PEO:E8:$NaIO_4$ = 63:27:10 wt%), was studied by electrochemical impedance spectroscopy. Relaxation characteristics for the polymer/liquid crystal PEO/E8/$NaIO_4$ composite were obtained, relevant to the applications of this ion-conducting dielectric material in flexible organic electronics and dielectric devices.

Keywords: flexible polymer electrolytes, liquid crystals, composites, Na^+-ion conducting polymer electrolytes, electrochemical impedance spectroscopy (EIS).

INTRODUCTION

Ion-transport solid and quasi-solid organic materials and electrolytes from polymers and liquid crystals (LCs) [1–5] are advanced materials that have an important role for the development of today's high-performance electrochemical and ionic devices, e.g., actuators, transducers, transistors, electrochromic devices, electrolyte membranes, as well as energy devices, such as batteries and capacitors, especially for flexible, portable and printed electronics [6–10]. Over the last decade, numerous studies have documented the use of ion transporters based on composites made from polymers and LCs, in particular ionic LCs [11–17]. Also, ion-conductor systems from polymers and nematic LCs (NLCs) have been developed and extensively studied [18–21] due to their important properties for practical use in flexible displays, flexible organic electronics and sensorics, solar-cell organic photovoltaics, as well as for rechargeable flexible mini-batteries and wearing electronics [22–25]. In this direction, the polymer poly(ethylene oxide) (PEO) and its derivatives were widely used as a polymer electrolyte matrix material for production of efficient ion-conducting systems [15, 26–29]. In particular, PEO-based sodium-ion (Na^+) conducting electrolytes were characterized with an easy processability and low cost, good electrochemical stability and compatibility with alkali salts, improved electrical properties and good ionic conductivity, which are vital for electrochemical and ionic devices [25, 30, 31].

Generally, the polymer/NLCs composites have attracted extensive research and application interest due to their unique electrical, dielectric, mechanical, and thermal properties [19, 20, 22, 23]. In addition, the blending of polymers with NLCs to produce ion-conducting electrolytes is considered as an effective method to modify also the properties of the polymers in such composites (e.g., the degree of crystallinity of the polymers), and thereby to enhance their ionic conductivity and other properties through intermolecular interaction between the polymers and NLCs [32]. This will be beneficial for future ionic device applications. Meanwhile, the selection of ion donor is paramount to enhance the ionic conductivity of the system. In this view, Na^+-based salts are found to give an excellent overall performance in terms of conductivity and stability, as the salts that contain Mg^{2+} ions. Furthermore, the use of Na ionic compounds can be an alternative to lithium-based salts (known to affect the environment). Our previous work reported a study of flexible films of Na^+-ion conducting composites from PEO with addition of molecules of the room-temperature NLCs with the commercial name E8 [32, 33]. Such ion-conductive electrolyte system attracted our attention because it exhibits ionic properties that are interesting for molecular electronics and soft-electronics applications. The structural and electrical conductivity investigations revealed an enhanced ionic and alternating-current (AC) conductivity, as well as other significant parameters, such as the amorphous and thermal properties of PEO/E8/$NaIO_4$ electrolyte films [32, 33], which contribute to their high performance, especially for future applications. Also, the effect of the molecules of E8 NLCs included in PEO/E8/$NaIO_4$ composites has been elucidated [32, 33]. Herein, the compositional ratio of the PEO/E8/$NaIO_4$ composite (w/w/w = 63/27/10

* To whom all correspondence should be sent:
E-mail: georgibh@issp.bas.bg

wt.%) was selected to be optimal due to the promising characteristics discussed earlier [32, 33]. Being of interest for the practical application of PEO/E8/$NaIO_4$ composite soft-solid dielectric materials, the present work is focusing on the study of their dielectric relaxation and ion conductivity relaxation in terms of (di)electric modulus, as depending on temperature. PEO/E8/$NaIO_4$ samples were characterized by means of electrochemical impedance spectroscopy in the frequency range 1 Hz – 1 MHz, in a room-temperature interval below their glass-transition temperature.

EXPERIMENTAL

Self-supported flexible films of the Na^+-ion conducting polymer/LC PEO/E8/$NaIO_4$ composite were prepared with the aid of standard solution cast technique. Details to materials, preparation, and experimental procedures using complex electrical impedance spectroscopy (EIS), as well as the morphological features and structural properties of the PEO/E8/$NaIO_4$ polymer-salt complexed composite material are given elsewhere [32]. The room-temperature NLC material E8 (commercial name, Merck) is a multi-component mixture of four cyanobiphenyl compounds: pentyl-cyanobiphenyl (5CB) and cyano-alkoxy-biphenyls (nOCB; n = 3; 5; 8), as well as pentyl-cyanoterphenyl (5CT). The weight percentage of these compounds in E8 is: 5CB (46 wt.%): 3OCB (16 wt.%), 5OCB (12 wt.%); 8OCB (16 wt.%); 5CT 5OCB (11 wt.%). The compositional ratio in the PEO/E8 blend was PEO:E8 = 70:30 (wt.%). The salt sodium metaperiodate ($NaIO_4$) was included in the polymer blend at a concentration of 10 wt.%. The frequency spectra of the complex electrical impedance of the films were measured by electrical impedance-meter Bio-Logic SP–200. The PEO/E8/$NaIO_4$ films were placed between two blocking electrodes of copper (area = 0.75 cm^2). The amplitude of the alternating-current (AC) voltage applied transversally to the films was 100 mV (sine function). The impedance spectra were recorded in the frequency range 1 Hz – 1 MHz. The measured impedance data has been transformed into electric modulus by using origin software. The temperature of the samples was maintained by a thermostat Mettler FP82 interfaced with a computer. The temperature accuracy was ± 0.1 °C. The impedimetric characteristics of the samples were obtained in the temperature range from 23 °C to 40 °C. This temperature interval is below the glass-transition temperature (42.5 °C) of PEO/E8/$NaIO_4$, as well as below the melting point (57.3 °C) for this composite [34]. The same applies for the phase-transition temperature from nematic to isotropic state for E8 LC (72 °C) [35].

RESULTS AND DISCUSSION

The experimental data for the complex electrical impedance $Z^* = Z' + i\,Z''$ obtained by EIS technique [36, 37] consist of both real (Z') and imaginary (Z'') parts of Z^* simultaneously measured as a function of the frequency f of the AC electric field applied on the sample. Fig. 1 shows the variation of frequency spectra of Z' and Z'' impedances for a sample of the considered PEO/E8/$NaIO_4$ composite electrolyte film at various temperatures.

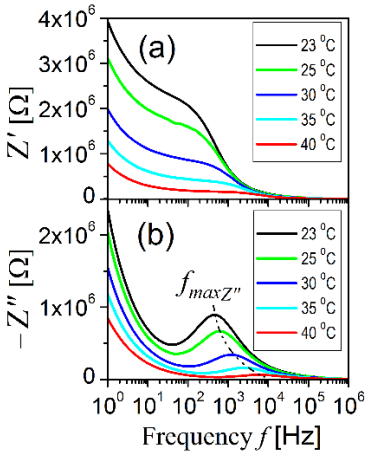

Fig. 1. Frequency-dependent real Z' (a) and imaginary Z'' (b) parts of complex electrical impedance of PEO/E8/$NaIO_4$ composite film at various temperatures.

The local maximum seen in $Z''(f)$ spectra (Fig. 1b) at frequency $f_{maxZ''}$ is related to the main dielectric relaxation in this dielectric material and is an indicator of its dipolar character. The shift of this maximum towards higher f is related to the increase of $f_{maxZ''}$ of the PEO/E8/$NaIO_4$ composite at elevating temperature. On the low-frequency side, the increase of the values of both Z' and Z'', seen at $f < 10$ Hz in our case, results from the well-known electrode polarization effect at the interface between the electrode and the sample. At low frequencies, this effect masks both electrical and dielectric properties of the studied dielectric material, in particular, the dielectric relaxation processes.

The ion conductivity relaxation in PEO/E8/$NaIO_4$ can be characterized with frequency spectra of complex (di)electric modulus (M^*) [38, 39]. By frequency spectra of M^* one can characterize the dielectric behavior and the conductivity relaxation of ion-conducting dielectric material. One advantage of modulus formalism is that in this way one can "unmask" the polarization effect from the bulk relaxation phenomenon at the interface between the electrode and dielectric sample (the above-mentioned effect from the electrode

interfacial polarization at low frequency), and thereby to observe the relaxation processes in a wide range of materials [38, 39].

Electric modulus M^* is defined as $M^* = 1/\varepsilon^*$, where ε^* is the complex dielectric permittivity function. The real (M') and imaginary (M'') parts of M^* are defined through the real (ε') and imaginary (ε'') parts of ε^* by expressions [38, 39]:

$$M' = \frac{\varepsilon'}{\varepsilon'^2 + \varepsilon''^2} \quad \text{and}$$

$$M'' = \frac{\varepsilon''}{\varepsilon'^2 + \varepsilon''^2} \qquad (1)$$

The complex impedance (Z^*) data can be transformed into complex electric modulus data, by using expressions [36]:

$$M' = -\frac{2\pi f \varepsilon_0 A}{l} Z'' \quad \text{and}$$

$$M'' = \frac{2\pi f \varepsilon_0 A}{l} Z' \qquad (2)$$

where ε_0 is the vacuum permittivity. In our case, l = 150 μm was the thickness of the film and A = 0.75 cm^2 was the contact area of the copper electrodes.

Fig. 2 presents the plots of the variation of the values of M' and M'' as a function of frequency at several temperatures, as calculated for the studied PEO/E8/$NaIO_4$ films by Eqs. (2). At low frequency, the modulus values approach zero at all temperature values indicating the effect of the electrode polarization phenomena. The lower values of the modulus result from enhanced capacitance. The relatively high value of capacitance is ascribed to the effective double layer charges building up at the interfacial region close to the blocking electrodes of the studied PEO/E8/$NaIO_4$ films. It is noticed in Fig. 2 (a) that the M' value continuously increases with the increase of frequency f in the range 1 Hz – 1 MHz and tends to saturate for higher frequencies. Such frequency-dependent behavior also takes place in the $M''(f)$ spectra (Fig. 2 b). In these plots, however, a peak is present, observed at a relatively high frequency $f_{max} \geq 100$ kHz (Fig. 2 b). This peak corresponds to a relaxation process and it is assigned to conductivity relaxation mechanism [38, 39]. The most probable conductivity relaxation time τ can be expressed as $\tau = 1/2\pi f_{max}$ [38, 39]. τ can be considered as the average time needed for the ions to transfer from a site to another site during the conduction process (in our case – ion hopping between ion coordination sites). The conductivity relaxation phenomenon is related to the lack of restoring force governing the mobility of charge carriers under the influence of an electric field [40]. This is attributed to conduction due to the short-range mobility of charge carriers.

As seen from Fig. 2 (b), on increasing temperature of the PEO/E8/$NaIO_4$ composite, the M'' peak at f_R shifts to higher frequencies. This signifies the faster movement of the mobile carriers of charge, in our case – the conducting ions (Na^+). The shifting of the peak in the M'' plots to higher frequency indicates that the relaxation time of the ions decreases as the temperature is raised. Such behavior is consistent with the enhanced polymer segmental motion at elevating temperature [41, 42]. Thus, the observed frequency shift of the M'' peak is directly related to the increase of ionic mobility and the increase of ionic conductivity, reported for the same PEO/E8/$NaIO_4$ composite on increasing temperature in the same range (23 – 40 °C) examined here [32]. The observed broadening of the relaxation peak in the $M''(f)$ spectra (Fig. 2 b) and its asymmetry are related to the spread of relaxation time. Such a broad nature of the peak can be interpreted as a consequence of the distribution of relaxation times τ and is an indication of the non-Debye type of relaxation behavior for the studied PEO/E8/$NaIO_4$ ion-conducting dielectric material.

Conductivity relaxation process that is characterized with a high relaxation frequency f_{max} at room temperature is a valuable property. This means that the dielectric material, in our case PEO/E8/$NaIO_4$ composite, is characterized with a fast ion migration up to this value of the frequency f_{max}.

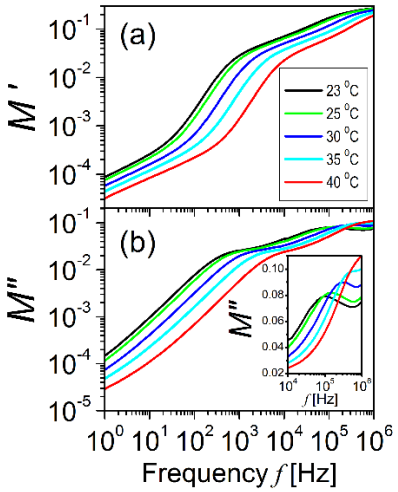

Fig. 2. Frequency spectra of: (a) real part (M'); (b) imaginary part (M'') of the complex electric modulus calculated for the studied PEO/E8/$NaIO_4$ composite film at various temperatures. Inset in (b): expanded view (10^4 – 10^6 Hz frequency range) for M'' in a linear scale.

Actually, of importance are two facts: (i) the relaxation frequency f_{max} of the ion conductivity of the studied electrolyte system is high (close to the

MHz range), and (ii) f_{max} becomes even higher with increasing temperature, i.e., under the same condition when both ion conductivity and dielectric properties of this composite are also improved [32]. Fig. 3 presents the cross-frequency (f_{cross}) characteristics of the electric modulus, i.e., the frequency at which M' is equal to M'', i.e., at f_{cross} $Z' = Z''$. It is noted that by increasing temperature, f_{cross} is increased (Fig. 3), like the frequency $f_{maxZ''}$ (Fig. 1 b). In both cases, this implies a dipolar character of the molecular interaction (dipole–dipole interaction) and a typical effect due to dipole relaxation as a result of heating of the PEO/E8/$NaIO_4$ polymer-based composite [41, 43]. By heating, a softening of the polymer PEO occurs, and thereby, the segmental motion of the polymer chains is enhanced. This leads to an increased relaxation frequency of PEO/E8/$NaIO_4$ flexible polymer/NLCs composite.

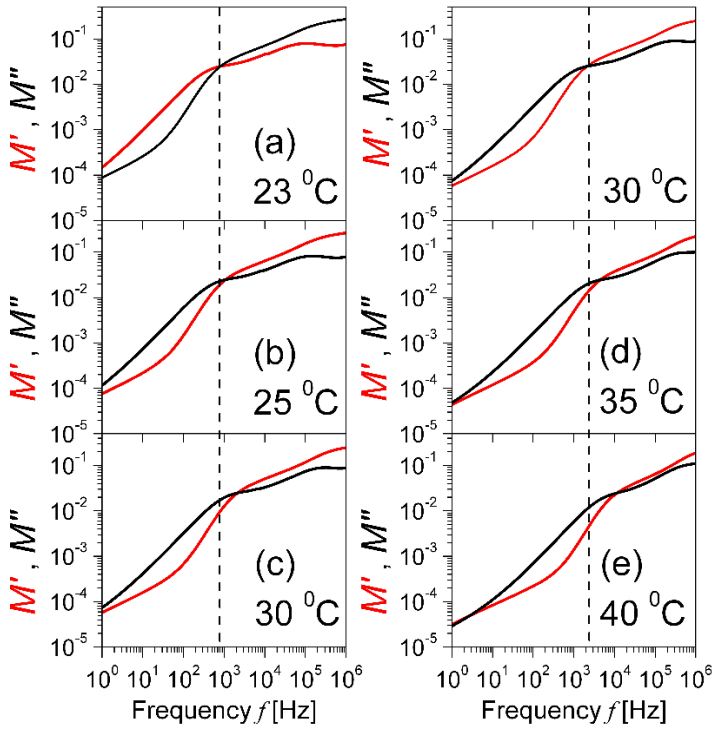

Fig. 3. The pairs of M' (red lines) and M'' (black lines) frequency spectra for PEO/E8/$NaIO_4$ composite at various temperatures (data from Fig. 2).

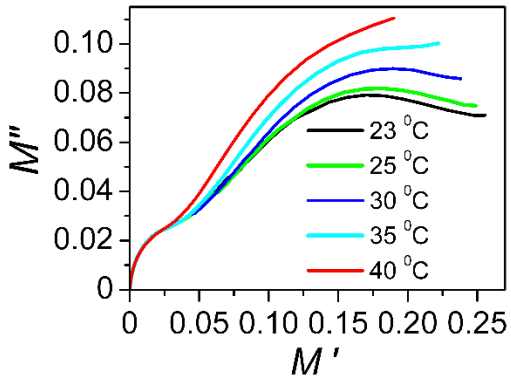

Fig. 4. M'' *vs* M' plots for the studied PEO/E8/$NaIO_4$ composite film.

Further, Argand (M'' *vs*. M') plots could be also used to characterize the mechanism of the relaxation dynamics. In our case, these plots do not exhibit a single semicircle (corresponding to a single relaxation) (Fig. 4) and this feature is due to the presence of two components in the composite –E8 LC and PEO. The results shown in Fig. 4 suggest that the almost non-dependent on temperature semicircle-like behaviors with a smaller diameter can be attributed to E8 LC, whereas the semicircular behaviors with a larger diameter correspond to the contribution of the polymer (PEO). The semicircles present for the Argand curves (above 35 °C they tend to form incomplete circles) reveal that the relaxation dynamics is due to conductivity relaxation. As such, the Argand curves calculated for PEO/E8/$NaIO_4$ significantly differ from the shapes (distorted arcs) typical for the relaxation mechanism corresponding to viscoelastic relaxation processes (or polymer molecular relaxation) found in multi-phase polymer-based systems and electrolytes [44, 45]. Commonly, a presence of a sharp peak in the M'' frequency spectrum accounts for the conductivity relaxation, whereas the viscoelastic relaxations typical for polymers are associated with a broad distribution of relaxation times [46]. Both types of relaxation in the studied PEO/E8/$NaIO_4$ composite are related to the

segmental motion of the main chain of the polymer (PEO), and the ion conductivity relaxation time τ decreases by increasing temperature in the same way as the viscosity. In our case, the results obtained by the M^* representations in Figs. 2 and 4 show that the conductivity relaxation as a factor determining the relaxation dynamics and ion transport properties of the studied PEO/E8/$NaIO_4$ composites is more important than the viscosity of the host polymer PEO.

CONCLUSIONS

The complex electric modulus of films of PEO/E8/$NaIO_4$ polymer/NLCs composite electrolyte system was studied to characterize the dielectric relaxation and ion conductivity relaxation in this flexible Na^+-ion conductor, examined by complex electrical impedance spectroscopy. The relaxation features (peaks) that occur in the imaginary parts of both electrical impedance (Z'') and electric modulus (M'') indicate the presence of orientation dipoles in PEO/E8/$NaIO_4$, which support the fast ion conduction. From frequency-domain electric modulus study the ion conductivity relaxation in PEO/E8/$NaIO_4$ can be deduced that has an important role for the ion transport. The ion conductivity relaxation is strongly influenced by the contribution of the polymer segmental relaxation in this polymer/NLCs composite system. The variation of the complex electric modulus with temperature and the increase of the relaxation frequency with the temperature, are ascribed to the enhanced polymer chain flexibility and corresponding increased ion mobility with temperature. The frequency spectra of the imaginary modulus $M''(f)$ used as an indicator of ion conductivity relaxation in PEO/E8/$NaIO_4$ composite, indicate that a quick response with a high ionic mobility can be achieved by this ion electrolyte. The results reported here show that the examined ion-conducting dielectric material is promising for ion electrolyte applications in flexible organic electronics and for use in dielectric devices. Moreover, the polymer/NLCs system considered here makes possible the employment of the unique properties of NLCs upon electro-magnetic fields (work in progress).

Acknowledgements: *We thank Dr. Hari Krishna Koduru from ISSP-BAS for providing us the PEO/E8/$NaIO_4$ samples, as well as for the helpful discussions. This work was supported by the Ministry of Education and Science of Bulgaria (MESB), through the National Science Fund of Bulgaria (research project No. KP-06-N58/6/2021). Todor Vlakhov gratefully acknowledges the support by the MESB under the National Research Programme "Young scientists and postdoctoral researches–2" approved by DCM 206/07.04.2022.*

REFERENCES

1. T. Kato, *Angew. Chem. Int. Ed.*, **49**, 7847 (2010).
2. V. K. Thakur, G. Ding, J. Ma, P. S. Lee, X. Lu, *Adv. Mater.*, **24**, 4071 (2012).
3. B. R. Wiesenauer, D. L. Gin, *Polym. J.*, **44**, 461 (2012).
4. J. Sakuda, E. Hosono, M. Yoshio, T. Ichikawa, T. Matsumoto, H. Ohno, H. Zhou, T. Kato, *Adv. Funct. Mater.*, **25**, 1206 (2015).
5. T. Kato, M. Yoshio, T. Ichikawa, B. Soberats, H. Ohno, M. Funahashi, *Nat. Rev. Mater.*, **2**, 17001 (2017).
6. A. J. Duncan, D. J. Leo, T. E. Long, *Macromolecules*, **41**, 7765 (2008).
7. S. H. Kim, K. Hong, W. Xie, K. H. Lee, S. Zhang, T. P. Lodge, C. D. Frisbie, *Adv. Mater.*, **25**, 1822 (2013).
8. X. Lu, M. Yu, G. Wang, Y. Tong, Y. Li, *Energy Environ. Sci.*, **7**, 2160 (2014).
9. I. Osada, H. De Vries, B. Scrosati, S. Passerini, *Angew. Chem. Int. Ed.*, **55**, 500 (2016).
10. H. Kokubo, R. Sano, K. Murai, S. Ishii, M. Watanabe, *Eur. Polym. J.*, **106**, 266 (2018).
11. M. Yoshio, T. Kato, in: Handbook of Liquid Crystals, J. W. Goodby, P. J. Collings, T. Kato, C. Tschierske, H. Gleeson, P. Raynes (eds.), Wiley-VCH, Weinheim, 2014, p. 727.
12. R. Sasi, S. Sarojam, S. J. Devaki, *ACS Sustainable Chem. Eng.*, **4**, 3535 (2016).
13. R. Sasi, B. Chandrasekhar, N. Kalaiselvi, S. J. Devaki, *Adv. Sustainable Syst.*, **1**, 1600031 (2017).
14. S. Wang, X. Liu, A. Wang, Z. Wang, J. Chen, Q. Zeng, X. Wang, L. Zhang, *Polym. Chem.*, **9**, 4674 (2018).
15. M. Zhang, A. Zhang, Q. Li, F. Li, S. Wang, S. Li, *J. Polym. Environ.*, **27**, 2369 (2019).
16. X. Chen, Y. Xie, Y. Ling, J. Zhao, Y. Xu, Y. Tong, S. Li, Y. Wang, *Mater. Design*, **192**, 108760 (2020).
17. Q. Zeng, Y. Lua, P. Chen, Z. Li, X. Wen, W. Wen, Y. Liu, S. Zhang, H. Zhao, H. Zhou, Z. X. Wang, L. Zhang, *J. Energy Chem.*, **67**, 157 (2022).
18. A. Z. S. B. Zulkifli, M. A. B. Kamarudin, A. B. Mainal, S. B. M. Said, *Adv. Mater. Res.*, **895**, 142 (2014).
19. S. M. Said, A. Z. S. Zulkifli, M. A. Kamarudin, A. Mainal, B. Subramanian, N. S. Mohamed, *Europ. Polym. J.*, **66**, 266 (2015).
20. S. M. Said, S. R. Sahamir, M. F. M. Sabri, M. A. Kamarudin, K. Hayashi, A. Z. S. Zulkifli, T. Nakajo, M. Kubouchi, Y. Miyazaki, *Molec. Cryst. Liq. Cryst.*, **642**, 9 (2017).
21. M. A. Kamarudin, A. A. Khan, S. M. Said, M. M. Qasim, T. D. Wilkinson, *Liq. Cryst.*, **45**, 112 (2018).
22. S. C. Kim, M. Song, T. I. Ryu, M. J. Lee, S.-H. Jin, Y.-S. Gal, H.-K. Kim, G.-D. Lee, Y. S. Kang, *Macromolec. Chem. Phys.*, **210**, 1844 (2009).

23. M. A. Karim, M. Song, J. S. Park, Y. H. Kim, M. J. Lee, J. W. Lee, C. W. Lee, Y. R. Cho, Y. S. Gal, J. H. Lee, S. H. Jin, *Dye Pigments*, **86**, 259 (2010).
24. M. A. A. Kamarudin, A. A. Khan, M. M. Qasim, T. D. Wilkinson, *Proc. SPIE,* **9940**, 994010 (2016).
25. H. K. Koduru, Y. G. Marinov, G. B. Hadjichristov, N. Scaramuzza, *Solid State Ionics*, **335**, 86 (2019).
26. J. Li, K. Kamata, M. Komura, T. Yamada, H. Yoshida, T. Iyoda, *Macromolecules*, **40**, 8125 (2007).
27. Y. Tong, L. Chen, X. He, Y. Chen, *Electrochim. Acta*, **118**, 33 (2014).
28. S. Wang, Q. Zeng, A. Wang, X. Liu, J. Chen, Z. Wang, L. Zhang, *J. Mater. Chem. A*, **7**, 1069 (2019).
29. J. D. Hwang, P. Y. Chen, S. W. Ding, C. W. Ong, *Crystals*, **9**, 627 (2019).
30. H. K. Koduru, L. Marino, F. Scarpelli, A. G. Petrov, Y. G. Marinov, G. B. Hadjichristov, M. T. Iliev, N. Scaramuzza, *Curr. Appl. Phys*., **17**, 1518 (2017).
31. G. B. Hadjichristov, Tz. E. Ivanov, Y. G. Marinov, H. K. Koduru, N. Scaramuzza, *Phys. Status Solidi (A): Appl. Mater. Sci.*, **216**, 1800739 (2019).
32. G. B. Hadjichristov, Y. G. Marinov, Tz. E. Ivanov, H. K. Koduru, N. Scaramuzza, in: Liquid and Single Crystals: Properties, Manufacturing and Uses, J. Goosen (ed.), Nova Science Publ., New York, 2020, p. 1.
33. G. Hadjichristov, Y. Marinov, A. Petrov, H. Koduru, N. Scaramuzza, *J. Phys. Conf. Ser.,* **1186**, 012020 (2019).
34. H. K. Koduru, Y. G. Marinov, F. Scarpelli, G. B. Hadjichristov, A. G. Petrov, N. Godbert, N. Scaramuzza, *J. Non-Crystal. Solids*, **499**, 107 (2018).
35. B. Bahadur, R. K. Sarna, V. G. Bhide, *Mol. Cryst. Liq. Cryst.*, **72**, 139 (1982).
36. V. F. Lvovich, Impedance Spectroscopy: Applications to Electrochemical and Dielectric Phenomena, John Wiley & Sons, Inc., Hoboken, 2012.
37. E. Barsoukov, J. R. Macdonald, Impedance Spectroscopy: Theory, Experiment, and Applications, Wiley, Hoboken, 2005.
38. P. B. Macedo, C. T. Moynihan, R. Bose, *Phys. Chem. Glasses,* **13**, 171 (1972).
39. A. K Jonscher, *J. Phys. D: Appl. Phys.*, **32,** R57 (1999).
40. I. M. Hodge, K. L. Ngai, C. T. Moynihan, *J. Non-Cryst. Solids*, **351**, 104 (2005).
41. C. H. Chan, H. W. Kammer, *Polymers*, **12**, 1009 (2020).
42. G. Polizos, E. Tuncer, V. Tomer, I. Sauers, C. A. Randall, E. Manias, in: Nanoscale Spectroscopy with Applications, S. M. Musa (ed.), CRC Press, Boca Raton, 2013, p. 93.
43. C. H. Chan, H. W. Kammer, *Pure Appl. Chem.*, **90**, 939 (2018).
44. A. S. Ayesh, *Chin. J. Polym. Sci.*, **28**, 537 (2010).
45. S. B. Aziz, W. O. Karim, M. A. Brza, R. T. Abdulwahid, S. R. Saeed, S. Al-Zangana, M. F. Z. Kadir, *Int. J. Mol. Sci.*, **20**, 5265 (2019).
46. K. Mohomed, T. G. Gerasimov, F. Moussy, J. P. Harmon, *Polymer*, **46**, 3847 (2005).